Dual Posttranscriptional Regulation via a Cofactor-Responsive mRNA Leader

Laura M. Patterson-Fortin[1],[†], **Christopher A. Vakulskas**[1],[†], **Helen Yakhnin**[2], **Paul Babitzke**[2], and **Tony Romeo**[1]

[1]**Department of Microbiology and Cell Science**, University of Florida, Gainesville, FL 32611-0700, USA

[2]**Department of Biochemistry and Molecular Biology**, Center for RNA Molecular Biology, Pennsylvania State University, University Park, PA 16802, USA

Abstract

Riboswitches are cis-acting mRNA elements that regulate gene expression in response to ligand binding. Recently, a class of riboswitches was proposed to respond to the molybdenum cofactor (Moco), which serves as a redox center for metabolic enzymes. The 5′ leader of the *Escherichia coli moaABCDE* transcript exemplifies this candidate riboswitch class. This mRNA encodes enzymes for Moco biosynthesis, and *moaA* expression is feedback inhibited by Moco. Previous RNA-seq analyses showed that *moaA* mRNA copurified with the RNA binding protein CsrA (carbon storage regulator), suggesting that CsrA binds to this RNA *in vivo*. Among its global regulatory roles, CsrA represses stationary phase metabolism and activates central carbon metabolism. Here, we used gel mobility shift analysis to determine that CsrA binds specifically and with high affinity to the *moaA* 5′ mRNA leader. Northern blotting and studies with a series of chromosomal *lacZ* reporter fusions showed that CsrA posttranscriptionally activates *moaA* expression without altering *moaA* mRNA levels, indicative of translation control. Deletion analyses, nucleotide replacement studies and footprinting with CsrA-FeBABE identified two sites for CsrA binding. Toeprinting assays suggested that CsrA binding causes changes in *moaA* RNA structure. We propose that the *moaA* mRNA leader forms an aptamer, which serves as a target of posttranscriptional regulation by at least two different factors, Moco and the protein CsrA. While we are not aware of similar dual posttranscriptional regulatory mechanisms, additional examples are likely to emerge.

Keywords

global regulation; translation control; molybdenum cofactor; riboswitch

Introduction

Posttranscriptional regulatory mechanisms govern gene expression at local (gene or operon specific) and global levels. The Csr (*c*arbon *s*torage *r*egulator) system of eubacteria is based on a small dimeric protein, CsrA or RsmA (repressor of stationary phase metabolites). In *Escherichia coli*, CsrA binds to hundreds of different mRNAs and regulates translation and transcript stability on a global scale.[1–3] While the regulatory consequences of most of the

Correspondence to Tony Romeo: tromeo@ufl.edu.
[†]L.M.P.-F. and C.A.V. contributed equally to this work.

RNA binding interactions of CsrA remain to be established, sequence-specific RNA binding by CsrA posttranscriptionally represses genes associated with stationary phase metabolism, nutrient stress responses and biofilm formation, while it activates genes for central carbon metabolism and motility.

The sequence GGA is a highly conserved central recognition element of CsrA binding sites, which may reside in unstructured RNA but, for optimal binding, is located in the loop of a stem–loop structure.[4,5] A consensus sequence for high-affinity binding, RUACARGGAUGU, was obtained by SELEX analysis.[5] CsrA-mediated repression often involves binding to a site overlapping the Shine–Dalgarno (SD) sequence and one or more other sites within the translation initiation region, thus preventing ribosome binding. Translational repression can also occur by CsrA altering mRNA structure or binding exclusively in the mRNA coding region.[6,7]

CsrA also binds to and activates expression of certain target mRNAs, for example, *flhDC*,[8] although no detailed activation mechanism has been established. Identical RNA binding surfaces are located on either side of the CsrA dimer and are composed of parallel β_1 and β_5 strands of the opposite polypeptides.[9–11]

Regulation of CsrA activity occurs at multiple levels.[3] Several CsrA dimers bind to small noncoding RNAs, CsrB and CsrC of *E. coli*, which sequester and antagonize this protein.[4,12,13] Transcription of these small RNAs is activated by the stringent response (ppGpp, DksA) and by acetate and shortchain carboxylates, which serve as a stimulus for the BarA/UvrY two-component signal transduction system.[14–16] Thus, CsrA activity can be decreased under limitation for amino acids or other nutrients and in the presence of carbon metabolism products. Turnover of CsrB/C requires ribonuclease E, polynucleotide phosphorylase and a specificity factor, CsrD, offering another point of regulation in this system.[17,18] CsrA levels are maintained under tight autoregulatory control, in which CsrA directly represses its own translation while indirectly activating its transcription.[19]

Riboswitches mediate cis-acting regulation and are formed by the three-dimensional folding of untranslated segments of mRNAs.[20,21] Riboswitches monitor and respond to physiological cues such as temperature, levels of specific nucleotides, amino acids, ions, cofactors and the proportional charging of tRNAs. Riboswitches are often composed of an aptamer domain, which binds to a specific ligand, and an expression platform, which controls downstream gene expression. Ligand binding causes structural changes affecting transcription termination, translation initiation or mRNA stability.[21,22] A few mRNAs respond to dual post-transcriptional regulatory factors, including tandem riboswitches recognizing the same[23,24] or different ligands[25] and an aptamer that binds to two molecules of the ligand.[26] mRNAs regulated both by a riboswitch and at a distinct location, by an RNA binding protein[27] or an antisense RNA[28] have also been reported. mRNA for the *Salmonella* Mg^{2+} transporter *mgtA* is regulated by a Mg^{2+}-sensing riboswitch and the effect of proline on a proline-rich open reading frame.[29,30] Nevertheless, prior to the present study, we were aware of no riboswitch aptamer that interacts with both a low-molecular-weight ligand and an RNA binding protein.

In *E. coli*, the guanine dinucleotide derivative of Moco forms the active site of redox enzymes involved in anaerobic carbon, sulfur and nitrogen metabolism.[31,32] Four operons, *moaABCDE*, *moeABC*, *mog* and *mobAB*, encode gene products needed for Moco biosynthesis; *modABCD* is required for molybdate uptake, and *modEF* genes encode a Mo-binding transcription factor and protein that may be involved in molybdate uptake, respectively.[33–38] Expression of the *moa* operon is activated by ModE and FNR transcription factors in response to molybdate availability and anaerobiosis,

respectively.[39,40] Genetic and bioinformatic evidence suggests that *moaA* transcription is feedback repressed by a riboswitch mechanism in which Moco binds to an RNA aptamer (Fig. 1) formed by the 5′ untranslated leader of this mRNA.[40–42]

Recent RNA-seq analyses identified hundreds of potential mRNA targets of CsrA binding in *E. coli*, including transcripts for molybdate uptake (*modA*), Moco biosynthesis (*moaA, moeA*) and Moco-dependent metabolism (*narL, narGHJI, nrfAEF, fdoGI, bisC, dmsA, fdnI, hyaA, napA* and *torZ*).[14] The present studies were conducted to determine whether CsrA binds directly to the proposed *moaA* riboswitch and how this affects *moaA* expression. We confirmed that CsrA binds specifically and with high affinity to the *moaA* mRNA leader and posttranscriptionally activates *moaA* expression. We propose that a single RNA aptamer mediates the regulatory effects of both CsrA and Moco on *moaA* expression. The physiological implication of these findings is that CsrA should enhance the cellular capacity for Moco biosynthesis under conditions of high metabolic demand.

Results

CsrA binds to the *moaA* mRNA leader

The *moaA* transcript was identified in RNA-seq analyses, along with >700 different *E. coli* mRNAs that copurified with CsrA.[14] To assess the basis of this observation, we used RNA gel mobility shift analysis to determine whether CsrA binds directly and specifically to the *moaA* leader (Fig. 1a). Mobility of the *moaA* mRNA leader extending from +1 to +134 was reduced upon incubation with increasing concentrations of purified CsrA-His$_6$ (Fig. 1b). Binding was observed beginning at 5 nM CsrA. A nonlinear least-squares analysis of the data revealed an apparent K_d value of 15 nM (Fig. 1d), which is within the range of affinities (4–40 nM) for other known mRNA targets of CsrA.[14,19,43] Binding specificity was demonstrated by competition assays in the presence of increasing concentrations of specific or nonspecific competitor RNAs. Addition of unlabeled specific competitor RNA (*moaA* RNA) competed with the formation of CsrA-*moaA* RNA complexes at the concentrations tested (Fig. 1c). In contrast, incubation with the *phoB* mRNA leader, which is not a direct target of CsrA binding,[44] did not compete for binding at these concentrations (Fig. 1c). Thus, CsrA binds to the *moaA* leader with high affinity and specificity.

To delineate the regions of the *moaA* mRNA leader required for CsrA interaction, we performed gel mobility shift analysis with a series of transcripts exhibiting stepwise 10-nt deletions from the 5′ or 3′ end. Deletions from the 5′ end, extending up to nucleotide +80, exhibited moderate, if any, effects on CsrA binding (Fig. 2). Thereafter, binding affinity decreased dramatically, consistent with the loss of an important binding site. In contrast, deletions from the 3′ end of this RNA drastically affected CsrA binding; an immediate reduction in CsrA-*moaA* complex formation was observed upon deletion of 10 nt (Fig. 2b). The CsrA-*moaA* RNA complexes that were observed at high CsrA concentrations (≥160 nM) appeared as broad smears, indicating that CsrA rapidly dissociated from the RNA during gel running, which reflects the low affinity of these complexes. Taken together, the deletion analyses indicated that the 3′ end of the *moaA* transcript leader is critical for CsrA binding, while the 5′ end up to approximately +80 nt is dispensable for high-affinity binding.

Positive footprinting of CsrA interaction with the *moaA* mRNA leader

Initial attempts to directly determine the CsrA binding sites of the *moaA* leader by nuclease protection assays were complicated by the extensive secondary structure of this RNA (data not shown). We therefore adapted a positive footprinting approach, FeBABE footprinting, in which a protein is modified by coupling to an Fe^{3+} chelate at cysteine residues, which upon reduction produces hydroxyl (•OH) radicals that react with DNA or RNA residues located

within a distance of up to 12 A from the FeBABE moiety, leading to strand scission.[45] Cysteine residues were singly introduced at two sites within the CsrA protein, Val8 and Ser41 (Fig. 3a). Val8 is located within the β_1 strand, which is critical for regulation and RNA binding, but Val8 itself is not essential for regulation[9] (Fig. 3b). Similarly, Ser41 is located in the β_5 strand, which is essential for RNA binding, but Ser41 itself is not critical for regulation.[9] Three specific cleavage sites in the *moaA* RNA were identified by this approach (Fig. 3). Footprinting with CsrA S41C-FeBABE protein caused cleavage at A90, U109 and A122 (Fig. 3c). Positions A90 and U109 were also cleaved in the presence of FeBABE-modified CsrA V8C (Fig. 3c). To validate this technique for mRNA footprinting, we performed a similar experiment on the *glgC* leader transcript, a minimally structured RNA that has been extensively characterized by RNase T1 and lead acetate footprinting, toeprinting and mutagenesis of the CsrA binding sites.[46] FeBABE footprinting using CsrA S41C yielded cleavages at four sites (A92, G94, A122 and A124), indicative of CsrA binding at two positions, which is consistent with the previous studies of CsrA binding to this transcript.[46] This observation validated the use of CsrA-FeBABE footprinting for analysis of CsrA binding to RNA.

CsrA binding examined by base substitutions

Analysis of the nucleotide sequences that were identified by deletion analyses and CsrA-FeBABE footprinting revealed two likely CsrA binding sites (Figs. 1–3). One site partially overlaps the stem of a previously determined hairpin, P4 (BS1),[41] while the other lies just upstream of the SD sequence (BS2). To determine whether either site is important for CsrA binding, we replaced the GG dinucleotide of each critical GGA by CC, which greatly reduces binding to authentic sites.[5] Substitutions at binding site BS1 (NT 91–92) allowed the formation of an initial complex with affinity similar to the CsrA-*moaA* wild-type (WT) RNA (compare Fig. 4a and b; 25 versus 28 nM). This was unexpected in view of the strong effects of deletions in this region (Fig. 2a), although the deletions likely caused more severe structural changes that interfered with CsrA binding. In contrast, substitutions in BS2 (NT 119–120) greatly reduced CsrA affinity for *moaA* RNA (BS2 M1; Fig. 4c and d). CsrA complexes with BS2 M1 RNA were only evident at <160 nM CsrA and appeared to be unstable, based on the appearance of a smear (Fig. 4d).

To determine whether the loss of CsrA binding in the BS2 mutant was due to a change in the primary sequence of a CsrA binding site or disruption of RNA secondary structure, we introduced compensatory base-pair substitutions to restore base pairing (Fig. 4c and e; BS2 M2). The latter substitutions did not further affect CsrA binding, suggesting that the loss of CsrA binding to the BS2 M1 RNA was caused by altering the sequence of this binding site and not simply by altering RNA secondary structure. These studies suggest that BS2 is necessary for high-affinity interaction of CsrA with *moaA* RNA, while BS1 may serve as a secondary site. Together, the BS1 and BS2 sequences appeared to fully account for CsrA binding to the *moaA* leader. It is noteworthy that the CsrA-FeBABE cleavage site at U109 (Fig. 3) was not associated with a conserved CsrA binding sequence and, most likely, does not represent an authentic binding site. Instead, U109 may lie close enough (within 12 A) to one of the two FeBABE moieties of the S41C CsrA dimer for a hydroxyl radical reaction to occur at this site when the protein interacts with the three-dimensional *moaA* mRNA. Indeed, in three-dimensional space, U109 is adjacent to the GGA motif of BS2 (Fig. 1e).

CsrA activates *moaA* expression

β-Galactosidase assays were performed to assess CsrA regulation of chromosomal translational and posttranscriptional fusions, *moaA '-'lacZ* and P*lacUV5-moaA '-'lacZ*, respectively (Fig. 5). Fusion expression was investigated under conditions in which the repressive effects of Moco were eliminated by growth in the presence of tungstate,

Na_2WO_4 [40,47]. Tungstate can replace molybdenum in the cofactor; however, the tungstate-bound cofactor does not mediate *moaA* repression.[40,41] Expression of the *moaA*'-'*lacZ* translational fusion showed a complex pattern with a maximum at the late exponential phase of growth. Disruption of CsrA decreased expression throughout the growth curve (Fig. 5b). Expression of the posttranscriptional fusion was driven by the constitutive *lacUV5* promoter to permit the effects of CsrA on the *moaA* leader to be determined in the absence of potential indirect effects of CsrA on *moaA* transcription. Disruption of the *csrA* gene also reduced expression of the P*lacUV5-moaA*'-'*lacZ* fusion (Fig. 5c and d). Ectopic expression of the *csrA* gene on a plasmid restored expression of this fusion to WT levels (Fig. 5d). These findings revealed that CsrA posttranscriptionally activates *moaA* expression.

Northern blotting to test for effects of CsrA on *moaABCDE* mRNA

Because CsrA protein is known to affect translation and/or stability of mRNAs,[1–3] Northern blotting was performed to assess the effect of CsrA on *moaABCDE* mRNA (Fig. 6). Total cellular RNA was isolated from WT and isogenic *csrA* mutant strains in the presence or absence of 20 mM tungstate (Na_2WO_4). Growth in the presence of Na_2WO_4 enhanced *moa* transcript accumulation in both WT and *csrA* mutant strains due to the loss of Moco-dependent repression under this condition.[40,41] Nevertheless, a *csrA* mutation did not affect *moa* mRNA accumulation in either the presence or the absence of tungstate. No transcript was detected in a *moaA::kan* mutant, confirming the specificity of this analysis. In conjunction with the finding that CsrA activates expression of the P*lacUV5-moaA-lacZ* posttranscriptional fusion (Fig. 6), these findings suggest that the effect of CsrA on *moaA* expression may be mediated entirely at the level of translation.

CsrA binding to *moaA* RNA examined by toeprinting

Toeprinting is a primer extension inhibition method that is used to identify the 3′ boundary of a bound protein or RNA structure. Toeprinting was used to identify RNA structures that form in the *moaA* leader, identify positions of bound CsrA, assess the effects of bound CsrA on RNA structure and determine if CsrA affects ribosome binding to *moaA* mRNA.[43] One distinct CsrA-dependent toeprint was observed at nucleotide 95 (TP9), consistent with CsrA binding at BS1 (Figs. 1e and 7). In addition, a nearby toeprint at nucleotide 99 (TP8) was lost upon CsrA binding. The latter observation is consistent with a structural change occurring in the loop of the P4 stem in response to CsrA binding. Perhaps bound CsrA disrupts an unusually stable GNRA tetraloop[48] that may form at the apex of the P4 stem (Figs. 1e and 7). No CsrA-dependent toeprint indicative of binding at BS2 was observed. However, a toeprint at nucleotide 112 (TP4) was reduced in the presence CsrA, which is consistent with CsrA-dependent disruption of pairing between the BS2 site (NT 119–120) and a complementary sequence (NT 110–111) in the *moaA* P5 stem.[41] We cannot explain the absence of a CsrA-dependent toeprint in response to binding at BS2. Perhaps the close proximity of the P1 stem to BS2 influences the processivity of reverse transcriptase in this region.

Most of the structural toeprints that occurred in the absence of CsrA were located at positions of secondary structure that were predicted by the original model of this RNA[41]: TP2 at NT 129, P1; TP3 at NT 120, P5; TP4 at NT 112, P5; TP5 and TP6 at NT 110 and NT 108, P4; TP8 at NT 99, P4 tetraloop; TP11 at NT 82, P3; TP12 at NT 66, P3; TP13 at NT 55, P2; TP14 at NT 48, P2; TP15 at NT 17, P1 (Figs. 1e and 7). Nevertheless, three toeprints, not predicted by the structural model, were observed: TP1 at NT 136, TP7 at NT 101 and TP10 at NT 86. Note that TP12 was not predicted by the original structure[41] but is consistent with an additional 2 bp of complementarity next to the terminal loop of P3, as shown in Fig. 1e.

The secondary structure that was modeled from in-line probing data of *moaA* RNA showed that the SD sequence is blocked by secondary structure in the absence of Moco.[41] Toeprint 2 (Figs. 1e and 7) is consistent with this model. Furthermore, toeprinting reactions with 30S ribosome subunits and tRNA[fMet] failed to produce a signal in the presence or absence of CsrA (data not shown). Controls using *glgC* mRNA as the template (data not shown) yielded the same 30S toeprint that was previously observed,[46] confirming that the 30S ribosomal subunits and tRNA[fMet] used in these studies were functional. Taken in context with gel shifts and footprinting analyses (Figs. 1–4), reporter fusion studies (Fig. 5) and Northern blotting (Fig. 6), these findings suggest that CsrA binding to *moaA* RNA is necessary but not sufficient to activate *moaA* translation.

Discussion

While CsrA has been known to regulate genes that function in aerobic carbon metabolism,[49–52] recent RNA-seq analyses of transcripts that copurify with CsrA identified many mRNAs that are necessary for anaerobic respiration, including the uptake of molybdate, biosynthesis of Moco and the production of Moco-dependent enzymes.[14] Here, we show that CsrA activates expression of *moaA*, which is needed for Moco biosynthesis. This positive regulatory role of CsrA is consistent with its known positive effects on genes of central metabolism, such as *pfkA, tpi* and *eno*, and its negative influence on genes such as *glgCAP, pfkB, fbp, pgm* and *cstA*, which are associated with secondary or stationary phase metabolism.[1,2,52] Nutritional stresses that trigger ppGpp synthesis or the accumulation of metabolic products, for example, acetate, activate transcription of the CsrB/C RNA antagonists of CsrA.[14,16] Thus, we propose that activation of *moaA* expression by CsrA serves to enhance the potential for Moco synthesis under nutritionally replete, anaerobic conditions. In addition to posttranscriptional regulation of *moaA* by Moco and CsrA, *moaA* transcription is activated by ModE and FNR in response to molybdate availability and anaerobiosis, respectively.[39,40] Thus, at least four regulatory mechanisms converge to govern *moaA* expression.

Our decision to study the effects of CsrA on *moaA* expression was based in part on evidence from Regulski *et al.* that the 5′ mRNA leader of this gene appears to serve as a Moco-responsive riboswitch, which mediates feedback repression on the Moco biosynthesis pathway.[41] Despite the fact that binding of Moco to *moaA* mRNA was not directly demonstrated due to the chemical instability of Moco, considerable genetic and bioinformatic evidence support this riboswitch model.[41] On the other hand, CsrA bound to *moaA* mRNA *in vivo*[14] and *in vitro* (Figs. 1–4 and 7) and posttranscriptionally activated *moaA* expression *in vivo* (Fig. 5). Furthermore, CsrA binding sites are located within the previously proposed Moco-specific aptamer.[41] To our knowledge, this is the first evidence for a riboswitch aptamer that is recognized by a regulatory protein in addition to a low-molecular-weight ligand.

The preferred CsrA binding sites contain a GGA triplet that is often, though not always, found within the single-stranded loop of a short hairpin structure.[4,5,9,10] Gel shift and FeBABE footprinting studies showed sequence-specific binding of CsrA at two predicted binding sites within the *moaA* 5′ leader (Figs. 1–4). The upstream CsrA binding site, BS1, is located within an unpaired segment of hairpin P4, whereas the downstream site, BS2, lies just upstream of the *moaA* SD sequence (Fig. 1). The effects of GG-to-CC dinucleotide substitutions at BS1 or BS2 implied that stronger binding occurs at BS2 (Fig. 4). Binding at BS2 may increase the local concentration of CsrA so that a single dimer might simultaneously interact with or bridge to a secondary site, BS1, at low CsrA concentrations, as previously shown for *glgC* mRNA.[10] Whether bridging actually occurs in *moaA* RNA or it is relevant for activation will require further study.

While negative regulation by CsrA has been extensively investigated, examples of positive regulation, as shown for *moaA*, are not well understood. CsrA-mediated repression often involves competition for mRNA binding with the ribosome. In these instances, the CsrA binding sites overlap the SD sequence, the initiation codon and/or the initial coding region.[1–3] A repression mechanism has also been identified in which mRNA binding by the CsrA homologue of *Pseudomonas aeruginosa*, RsmA, alters RNA structure by stabilizing base-pairing interactions between the SD sequence and an anti-SD sequence.[6] Negative regulation of translation is frequently, though not always, associated with decreased mRNA stability. A priori, CsrA might activate gene expression by effects on translation, mRNA stability or a combination of the two. CsrA activates *flhDC* expression by binding to the *fhlDC* mRNA leader and stabilizing it, possibly by blocking RNase-E-mediated cleavage[3,8] (unpublished results). Because CsrA activated a *moaA* posttranscriptional reporter fusion (Fig. 5) and did not affect *moaABCDE* mRNA levels (Fig. 6), *moaA* appears to represent the first example in which CsrA activates translation.

An existing model of *moaA* mRNA leader regulation proposes that binding of Moco to the *moaA* mRNA leader alters its structure in a way that affects transcription of the entire *moaABCDE* operon.[40–42] Our Northern blotting studies supported this idea (Fig. 6), although the way in which this occurs still remains to be determined.

Nucleotide substitution studies provided evidence for high-affinity binding of CsrA at BS2, which is located just upstream from the *moaA* SD sequence (Figs. 1 and 4). Furthermore, a toeprint (TP4) that is consistent with the P5 stem overlaps BS2. This toeprint found to decrease upon CsrA binding, implying that a loss of secondary structure is necessary for binding at BS2 (Figs. 1e and 7). On the other hand, no CsrA-dependent toeprint was observed at BS2 (Figs. 1 and 7). While the latter result remains unexplained, it may reflect a scenario in which a CsrA toeprint at BS2 is masked by the effects of the proximal P1 stem (at the SD sequence) on reverse transcriptase progress in this segment of RNA.

We have been unable to demonstrate *in vitro* activation of *moaA* expression by CsrA in a coupled transcription–translation system, and we did not observe a toeprint for the 30S ribosomal subunit on *moaA* RNA (data not shown). Controls for each of these reactions, conducted in parallel using *glgC* as a model, revealed that CsrA and the 30S ribosomal subunit were functional in these *in vitro* assays, as reported previously.[46,53] Because translational regulation by CsrA has been observed for many mRNAs, including *glgC, pgaA, cstA, sdiA* and *csrA* itself[7,19,46,54,55] using *in vitro* assays, it seems that *moaA* translation may involve additional factors that were not present or not active in the reactions.

Along with the chemical instability of Moco,[41] the apparent inability to translate *moaA* mRNA *in vitro* dictates that fundamental questions about posttranscriptional regulation via the *moaA* mRNA leader must await further advances: Does Moco actually bind to *moaA* RNA, and if so, how does this affect *moaABCDE* mRNA levels? What other factors or conditions are required in addition to CsrA for facilitating translation of *moaA*, and how is this accomplished? Does Moco binding prevent CsrA from interacting with this RNA, or might both factors bind simultaneously? Progress in answering these questions will advance our basic understanding of the diverse processes and mechanisms that have evolved for carrying out posttranscriptional regulation.

Materials and Methods

Bacterial strains, bacteriophage, plasmids and growth conditions

All *E. coli* K12 strains, plasmids and bacteriophage used in this study are listed in Table 1. Bacterial cultures were grown in LB medium at 37 °C and aerated by shaking at 250 rpm.

Glycogen accumulation was assessed with iodine vapor staining of bacteria grown on Kornberg medium [1.1% K_2HPO_4, 0.85% KH_2PO_4, 0.6% yeast extract, 1% glucose (pH 6.8) and 1.5% agar].[49] Antibiotics were added where appropriate, at the following concentrations: ampicillin, 100 μg/ml; kanamycin, 200 μg/ml; tetracycline, 10 μg/ml.

RNA electrophoretic mobility shift assays

Quantitative mobility shifts were performed as previously described.[60] *E. coli* CsrA-His$_6$ was expressed and purified as previously described.[9] DNA templates for RNA synthesis were generated by PCR amplification of CF7789 genomic DNA or by annealing of complementary oligonucleotides (Table 2). RNA templates were synthesized *in vitro* using the MEGAshortscript kit (Ambion) and purified by denaturing gel electrophoresis. Purified RNA transcripts were dephosphorylated with Antarctic Phosphatase (New England Biolabs) and subsequently end-labeled with [-^{32}P]ATP and T4 polynucleotide kinase (Ambion) and purified by denaturing gel electrophoresis. Binding reactions were performed for 30 min at 37 °C in 1× binding buffer [10 mM Tris–HCl (pH 7.5), 10 mM $MgCl_2$ and 100 mM KCl], 3.25 ng total yeast RNA, 20 mM DTT, 7.5% glycerol, 4 U SUPERasin (Ambion), 80 pM radiolabeled RNA and the indicated protein concentration in a final volume of 10 μl. Reaction products were separated on Tris–borate–ethylenediaminetetraacetic acid (EDTA) non-denaturing polyacrylamide gels and analyzed by phosphorimaging. Bound and unbound RNA species were quantified with Quantity One (Bio-Rad), and an apparent equilibrium binding constant (K_d) was calculated as previously described.[9] Competition assays were performed to control for nonspecific protein binding. The nonspecific, unlabeled competitor RNA, *phoB*, was generated as described above using annealed primers phoBT7-F and phoBT7-R.

Generation of base-substituted *moaA* RNAs

The *moaA* plasmid, pAltermoaA, was generated by PCR amplification of the *moaA* leader extending from +4 to +144 using primer pair LPF-85/LPF-86 (Table 2). Purified DNA was digested with EcoRI and BamHI and cloned into EcoRI and BamHI digested pAlt-C4 plasmid DNA.[53] The resulting plasmid, pAltermoaA, was used as template to introduce base-pair changes within putative CsrA binding sites of the *moaA* leader using the QuikChange II XL kit (Stratagene). The mutations were confirmed by sequence analysis.

Construction of templates for cysteine-substituted CsrA by site-directed mutagenesis

The WT CsrA protein contains no cysteine. Thus, two CsrA-His$_6$ proteins with single cysteine substitutions at V8 and S41, suitable for FeBABE conjugation, were created and expressed from derivatives of plasmid pCSRH6-19 or pCSB12. The QuikChange II XL kit (Stratagene) was used, as instructed by the manufacturer, to construct the mutant plasmids. Oligonucleotides for the mutagenesis reactions are listed in Table 2; changes to the DNA sequence, shown in boldface, were confirmed by sequence analysis. Functionality of the mutant genes was confirmed by their ability to complement the effect of a *csrA::kan* mutation on glycogen biosynthesis.[9]

Modeling of the three-dimensional structure of CsrA

Coordinates for the modeling of the *Yersinia enterocolitica* CsrA protein (Protein Data Bank ID 2BTI) were rendered using the Cn3D macromolecular structure viewer.[61]

CsrA-His$_6$ protein purification

Cysteine mutant proteins were expressed and purified as previously described for WT CsrA-His$_6$[9] with the addition of a heparin column purification step. Ni-NTA fractions containing the CsrA-His$_6$ mutant proteins were diluted 4-fold in Buffer A [50 mM sodium phosphate

(pH 7.0) and 100 mM NaCl] and loaded onto a HiTrap Heparin HP column (GE Healthcare). The column was washed with Buffer A, and bound protein was eluted by a linear gradient of Buffer A containing 100 mM to 2 M NaCl. Column fractions were analyzed by 15% SDS-PAGE analysis and Coomassie Blue Staining. Fractions containing CsrA protein (>95% purity) were combined and concentrated using Amicon centrifugal filter units. Binding to the *moaA* untranslated leader RNA by the cysteine-substituted and WT proteins was indistinguishable in gel shifts.

FeBABE modification of single cysteine mutants of CsrA

Proteins for FeBABE [*p*-bromoacetamidobenzyl-EDTA, iron(III) chelate] conjugation were treated consecutively with DTT (1 mM) and EDTA (20 mM) for 5 min at room temperature. Proteins were dialyzed at 4 °C against conjugation buffer [30 mM Mops, 100 mM NaCl, 1 mM EDTA (pH 8.0) and 5% glycerol]. Dialyzed protein was mixed with a 20-fold molar excess reconstituted FeBABE reagent (8.5 nM; Thermo Scientific), and the conjugation reaction was performed in the dark for 2 h at room temperature with gentle mixing. Unconjugated FeBABE was removed by dialysis against conjugation buffer. The extent of conjugation was analyzed by determining concentration of remaining free sulfhydryl groups using Ellman's Reagent (Thermo Scientific). Concentrated FeBABE conjugated proteins were stored at −80 °C.

FeBABE footprinting

Footprinting reactions were performed for 30 min at 37 °C in 1× binding buffer [10 mM Tris–HCl (pH 7.5), 10 mM $MgCl_2$ and 100 mM KCl], 3.25 ng total yeast RNA, 5% glycerol, 4 U SUPERasin (Ambion), 500 pM 5 radiolabeled RNA and the indicated protein concentration in a final volume of 20 µl. RNAs were prepared as described above except that linearized pAlt-C4 plasmid DNA was used as the template for transcription of the *glgC* mRNA leader.[53] RNA cleavage was initiated by the addition of ascorbic acid (5 mM ascorbic acid and 1.25 mM EDTA at pH 8.0) and hydrogen peroxide solution (5 mM hydrogen peroxide and 1.25 mM EDTA at pH 8.0) followed by 1 min of incubation at 37 °C. Reactions were quenched with 0.1 M thiourea and ethanol precipitated. Precipitated RNA was resuspended in formamide loading buffer (95% formamide, 10 mM NaOH, 0.05% xylene cyanol and 0.05% bromophenol blue), separated on a 5% sequencing gel and analyzed using a phosphorimager. Partial alkaline hydrolysis and RNase T1 ladders were prepared as previously described.[46,48]

Toeprinting of the *moaA* mRNA leader

Toeprint assays followed a previously published procedure with minor modifications.[62] *E. coli* 30S ribosomal subunits were purified as previously described.[46] The DNA template for *in vitro* transcription was a PCR product containing the *moaA* leader and the first 14 bp of the *moaA* coding sequence fused in-frame with *lacZ*. This DNA template was amplified using pMoaA (*moaA* '-'*lacZ* translational fusion cloned between the PstI and BamHI sites of pLFT[14]) as a template and T7 MoaA-For and LacZ2 primers. A 228-nt RNA (+3 to +144 nt relative to the transcriptional start of *moaA*, a BamHI site at the *moaAlacZ* junction and 87 nt of the *lacZ* coding sequence) was synthesized *in vitro* using the RNAMaxx High Yield Transcription kit (Agilent Technologies). Gel-purified RNA from this fusion, in Tris–EDTA buffer, was hybridized to a 5 -end-labeled primer (LacZ2) that was complementary to the 3 end of the transcript by heating at 80 °C for 3 min, followed by slow cooling to room temperature. Toeprint reaction mixtures (10 µl) contained 2 µl of the hybridization mixture (the final concentration of the RNA and the oligonucleotide was 15 nM), 2 µM CsrA-His_6 and/or 150 nM 30S ribosomal subunits with or without 5 µM $tRNA^{fMet}$, 375 µM each deoxynucleoside triphosphate and 10 mM DTT in toeprint buffer [10 mM Tris–HCl (pH 7.4), 10 mM $MgCl_2$ and 60 mM ammonium acetate]. Previously frozen 30S ribosomal

subunits were thawed and activated by incubation at 37 °C for 15 min. Mixtures containing CsrA were incubated at 37 °C for 30 min to allow CsrA-mRNA complex formation, prior to the addition of 30S subunits. 30S ribosomal subunit toeprint reactions were performed by incubating RNA, 30S ribosomal subunits with or without tRNA[fMet], in toeprint buffer as described previously.[63] Following the addition of 0.1–0.5 U of SuperScript III reverse transcriptase (Invitrogen) or 0.05–0.2 U of avian myeloblastosis virus reverse transcriptase (New England Biolabs), we incubated the reaction mixture at 37 °C for 15 min. Reactions were terminated by the addition of 6 μl of formamide-containing loading buffer. Samples were heated for 2 min at 90 °C prior to fractionation through standard 6% polyacrylamide sequencing gels. Radioactive bands were visualized using a phosphorimager.

Northern blotting

E. coli cultures were grown to an OD_{600} of 0.8–1.0 in LB medium supplemented with 20 mM sodium tungstate (as indicated), and total cellular RNA was isolated using the RNeasy mini kit according to manufacturer's instructions (QIAGEN). Total cellular RNA was separated on a 1.2% agarose formaldehyde gel and transferred to a positively charged nylon membrane (Roche Diagnostics) by electro-blotting using the Mini Trans-Blot Cell (Bio-Rad). RNA was fixed to the membrane by UV cross-linking. Blots were hybridized overnight at 68 °C with a DIG-labeled antisense *moaA* RNA probe using the DIG Northern Starter kit (Roche Diagnostics) according to manufacturer's instructions. The antisense *moa* RNA probe encompassing the entire *moaA* open reading frame was transcribed *in vitro* using the DIG Northern Starter kit (Roche Diagnostics) from a PCR product that was generated using the primer pair ASmoaAT7for and ASmoaAT7rev (Table 2). Blots were developed using the ChemiDoc XRS+ system (Bio-Rad) and quantified using Quantity One image analysis software (Bio-Rad).

Construction of chromosomal *moaA'-'lacZ* and P*lacUV5-moaA'-'lacZ* translational fusions

The *moaA* reporter fusions, *moaA'-'lacZ* and P*lacUV5-moaA'-'lacZ* were generated by PCR amplification of the upstream regulatory region of *moaA* extending from −253 to +155 and from +4 to +155 relative to the start of transcription, respectively. Primer pairs for PCR amplification are listed in Table 2. Purified DNAs were digested with PstI and BamHI and cloned into PstI and BamHI digested pLFT plasmid DNA.[14] The resulting plasmids, pmoaA and pUV5moaA, were sequenced to confirm successful in-frame insertion of the *moaA* insert. Fusions were integrated into the chromosome of CF7789 or MC CF7789 as previously described.[57]

β-Galactosidase and total protein assays

-Galactosidase experiments were performed as previously described.[14] All experiments were performed in triplicate. Total cellular protein was measured using the bicinchoninic acid assay (Pierce Biotechnology) with bovine serum albumin as the protein standard.

Acknowledgments

Abbreviations used

SD   Shine–Dalgarno

WT   wild type

EDTA   ethylenediaminetetraacetic acid

References

1. Romeo T. Global regulation by the small RNA binding protein CsrA and the noncoding RNA CsrB. Mol. Microbiol. 1998; 29:321–1330. [PubMed: 9701824]

2. Babitzke P, Romeo T. CsrB sRNA family: sequestration of RNA-binding regulatory proteins. Curr. Opin. Microbiol. 2007; 10:156–163. [PubMed: 17383221]

3. Romeo T, Vakulskas CA, Babitzke P. Posttranscriptional regulation on a global scale: form and function of Csr/Rsm systems. Environ. Microbiol. 2012 [Epub ahead of print].

4. Liu MY, Gui G, Wei B, Preston JF III, Oakford L, Yuksel U, et al. The RNA molecule CsrB binds to the global regulatory protein CsrA and antagonizes its activity in *Escherichia coli*. J. Biol. Chem. 1997; 272:17502–17510. [PubMed: 9211896]

5. Dubey AK, Baker CS, Romeo T, Babitzke P. RNA sequence and secondary structure participate in high-affinity CsrA–RNA interaction. RNA. 2005; 11:1579–1587. [PubMed: 16131593]

6. Irie Y, Starke M, Edwards AN, Wozniak DJ, Romeo T, Parsek MR. *Pseudomonas aeruginosa* biofilm matrix polysaccharide Psl is regulated transcriptionally by RpoS and posttranscriptionally by RsmA. Mol. Microbiol. 2010; 78:158–172. [PubMed: 20735777]

7. Yakhnin H, Baker CS, Berezin I, Evangelista MA, Rassin A, Romeo T, Babitzke P. CsrA represses translation of *sdiA*, encoding the *N*-acylhomoserine-l-lactone receptor of *Escherichia coli* by binding exclusively within the coding region of *sdiA* mRNA. J. Bacteriol. 2011; 193:6162–6170. [PubMed: 21908661]

8. Wei BL, Brun-Zinkernagel AM, Simecka JW, Pruss BM, Babitzke P, Romeo T. Positive regulation of motility and *fhlDC* expression by the RNA-binding protein CsrA of *Escherichia coli*. Mol. Microbiol. 2001; 40:245–256. [PubMed: 11298291]

9. Mercante J, Suzuki K, Cheng X, Babitzke P, Romeo T. Comprehensive alanine-scanning mutagenesis of *Escherichia coli* CsrA defines two subdomains of critical functional importance. J. Biol. Chem. 2006; 281:31832–31842. [PubMed: 16923806]

10. Mercante J, Edwards AE, Dubey AK, Babitzke P, Romeo T. Molecular geometry of CsrA (RsmA) binding to RNA and its implications for regulated expression. J. Mol. Biol. 2009; 392:511–528. [PubMed: 19619561]

11. Schubert M, Lapouge K, Duss O, Oberstrass FC, Jelesarov I, Haas D, Allain FH. Molecular basis of messenger RNA recognition by the specific bacterial repressing clamp RsmA/CsrA. Nat. Struct. Mol. Biol. 2007; 14:807–813. [PubMed: 17704818]

12. Suzuki K, Wang X, Weilbacher T, Pernestig AK, Melefors O, Georgellis D, et al. Regulatory circuitry of the CsrA/CsrB and BarA/UvrY systems of *Escherichia coli*. J. Bacteriol. 2002; 184:5130–5140. [PubMed: 12193630]

13. Weilbacher T, Suzuki K, Dubey AK, Wang X, Gudapaty S, Morozov I, et al. A novel sRNA component of the carbon storage regulatory system of *Escherichia coli*. Mol. Microbiol. 2003; 48:657–670. [PubMed: 12694612]

14. Edwards AN, Patterson-Fortin LM, Vakulskas CA, Mercante JW, Potrykus K, Vinella D, et al. Circuitry linking the Csr and stringent response global regulatory systems. Mol. Microbiol. 2011; 80:1561–1580. [PubMed: 21488981]

15. Jonas K, Melefors O. The *Escherichia coli* CsrB and CsrC small RNAs are strongly induced during growth in nutrient-poor medium. FEMS Microbiol. Lett. 2009; 297:80–86. [PubMed: 19538511]

16. Chavez RG, Alvarez AF, Romeo T, Georgellis D. The physiological stimulus for the BarA sensor kinase. J. Bacteriol. 2010; 192:2009–2012. [PubMed: 20118252]

17. Suzuki K, Babitzke P, Kushner SR, Romeo T. Identification of a novel regulatory protein (CsrD) that targets the global regulatory RNAs CsrB and CsrC for degradation by RNase E. Genes Dev. 2006; 20:2605–2617. [PubMed: 16980588]

18. Jonas K, Edwards AN, Ahmad I, Romeo T, Romling U, Melefors O. Complex regulatory network encompassing the Csr, c-di-GMP and motility systems of *Salmonella Typhimurium*. Environ. Microbiol. 2010; 12:524–540. [PubMed: 19919539]

19. Yakhnin H, Yakhnin AV, Baker CS, Sineva E, Berezin I, Romeo T, Babitzke P. Complex regulation of the global regulatory gene *csrA*: CsrA-mediated translational repression, transcription from five promoters by E [70] and E [S]. Mol. Microbiol. 2011; 81:689–704. [PubMed: 21696456]

20. Henkin TM. Riboswitch RNAs: using RNA to sense cellular metabolism. Genes Dev. 2008; 22:3383–3390. [PubMed: 19141470]

21. Roth A, Breaker RR. The structural and functional diversity of metabolite-binding riboswitches. Annu. Rev. Biochem. 2009; 78:305–334. [PubMed: 19298181]

22. Grundy FJ, Henkin TM. From ribosome to ribowitch: control of gene expression in bacteria by RNA structural rearrangements. Crit. Rev. Biochem. Mol. Biol. 2006; 41:329–338. [PubMed: 17092822]

23. Mandal M, Lee M, Barrick JE, Weinberg Z, Emilsson GM, Ruzzo WL, Breaker RR. A glycine-dependent riboswitch that uses cooperative binding to control gene expression. Science. 2004; 306:275–279. [PubMed: 15472076]

24. Welz R, Breaker RR. Ligand binding and gene control characteristics of tandem riboswitches in Bacillus anthracis. RNA. 2007; 13:573–582. [PubMed: 17307816]

25. Sudarsan N, Hammond MC, Block KF, Welz R, Barrick JE, Roth A, Breaker RR. Tandem riboswitch architectures exhibit complex gene control functions. Science. 2006; 314:300–304. [PubMed: 17038623]

26. Trausch JJ, Ceres P, Reyes FE, Batey RT. The structure of a tetrahydrofolate-sensing riboswitch reveals two ligand binding sites in a single aptamer. Structure. 2011; 19:1413–1423. [PubMed: 21906956]

27. Fox KA, Ramesh A, Stearns JE, Bourgogne A, Reyes-Jara A, Winkler WC, Garsin DA. Multiple posttranscriptional regulatory mechanisms partner to control ethanolamine utilization in *Enterococcus faecalis*. Proc. Natl Acad. Sci. USA. 2009; 106:4435–4440. [PubMed: 19246383]

28. André, G., Even S, Putzer H, Burgière P, Croux C, Danchin A, et al. S-box and T-box riboswitches and antisense RNA control a sulfur metabolic operon of *Clostridium acetobutylicum*. Nucleic Acids Res. 2008; 36:5955–5969. [PubMed: 18812398]

29. Cromie MJ, Shin Y, Latifi T, Groisman EA. An RNA sensor for intracellular Mg^{2+} Cell. 2006; 125:71–84. [PubMed: 16615891]

30. Park S-Y, Cromie MJ, Lee E-J, Groisman EA. A bacterial mRNA leader that employs different mechanisms to sense disparate intracellular signals. Cell. 2010; 142:737–748. [PubMed: 20813261]

31. Schwarz G, Mendel RR. Molybdenum cofactor biosynthesis and molybdenum enzymes. Annu. Rev. Plant Biol. 2006; 57:18343–18350.

32. Schwarz G. Molybedenum cofactor biosynthesis and deficiency. Cell. Mol. Life Sci. 2005; 62:2792–2810. [PubMed: 16261263]

33. Nohno A, Kasai Y, Saito T. Cloning and complete nucleotide sequence of the *Escherichia coli chlEN* operon involved in molybdopterin biosynthesis. J. Bacteriol. 1988; 170:4097–4102. [PubMed: 3045084]

34. Johnson JL, Indermaur LW, Rajagopalan KV. Molybdenum cofactor biosynthesis in *Escherichia coli*: requirement of the *chlB* gene product for the formation of the molybdopterin guanine dinucleotide. J. Biol. Chem. 1991; 266:12140–12145. [PubMed: 1648082]

35. Rajagopalan KV, Johnson JL. The pterin molybdenum cofactors. J. Biol. Chem. 1992; 267:10199–10202. [PubMed: 1587808]

36. Iobi-Nivol C, Palmer T, Whitty PW, McNairn E, Boxer DH. The *mob* locus of *Escherichia coli* K12 required for molybdenum cofactor biosynthesis is expressed at very low levels. Microbiology. 1995; 141:1663–1671. [PubMed: 7551035]

37. Maupin-Furlow JA, Rosentel JK, Lee JH, Deppenmeier U, Gunsalus RP, Shanmugam KT. Genetic analysis of the *modABCD* (molybdenum transport) operon of *Escherichia coli*. J. Bacteriol. 1995; 177:4851–4856. [PubMed: 7665460]

38. Rech S, Deppenmeier U, Gunsalus RP. Regulation of the molybdate transport operon, *modABCD*, of *Escherichia coli* in response to molybdate availability. J. Bacteriol. 1995; 177:1023–1029. [PubMed: 7860583]

39. McNicholas PM, Rech SA, Gunsalus RP. Characterization of the ModE DNA-binding sites in the control regions of *modABCD* and *moaABCDE* of *Escherichia coli*. Mol. Microbiol. 1997; 23:515–524. [PubMed: 9044285]

40. Anderson LA, McNairn E, Leubke T, Pau RN, Boxer DH. ModE-dependent molybdate regulation of the molybdenum cofactor operon *moa* in *Escherichia coli*. J. Bacteriol. 2000; 182:7035–7043. [PubMed: 11092866]

41. Regulski EE, Moy RH, Weinberg Z, Barrick JE, Yao Z, Ruzzo WL, Breaker RR. A widespread riboswitch candidate that controls bacterial genes involved in molybdenum cofactor and tungsten cofactor metabolism. Mol. Microbiol. 2008; 68:918–932. [PubMed: 18363797]

42. Baker KP, Boxer DH. Regulation of the *chlA* locus of *Escherichia coli* K12: involvement of molybdenum cofactor. Mol. Microbiol. 1991; 5:901–907. [PubMed: 1906967]

43. Pannuri A, Yakhnin H, Vakulskas CA, Edwards AN, Babitzke P, Romeo T. Translational repression of NhaR, a novel pathway for multi-tier regulation of biofilm circuitry by CsrA. J. Bacteriol. 2012; 194:79–89. [PubMed: 22037401]

44. Edwards, AN. Ph.D. Dissertation. Emory University; Atlanta, GA: 2010. The global regulatory role of the RNA binding protein CsrA.

45. Heilek GM, Marusak R, Meares CF, Noller HF. Directed hydroxyl radical probing of 16S rRNA using Fe(II) tethered to ribosomal protein S4. Proc. Natl Acad. Sci. USA. 1995; 92:1113–1116. [PubMed: 7862644]

46. Baker CS, Morozov I, Suzuki K, Romeo T, Babitzke P. CsrA regulates glycogen biosynthsis by preventing translation of *glgC* in *Escherichia coli*. Mol. Microbiol. 2002; 44:1599–1610. [PubMed: 12067347]

47. Kletzin A, Adams MW. Tungsten in biological systems. FEMS Microbiol. Rev. 1996; 18:5–63. [PubMed: 8672295]

48. Bevilacqua JM, Bevilacqua PC. Thermodynamic analysis of an RNA combinatorial library contained in a short hairpin. Biochemistry. 1998; 37:15877–15884. [PubMed: 9843393]

49. Romeo T, Gong M, Liu MY, Brun-Zinkernagel AM. Identification and molecular characterization of *csrA*, a pleiotropic gene from *Escherichia coli* that affects glycogen biosynthesis, gluconeogenesis, cell size, and surface properties. J. Bacteriol. 1993; 175:4744–4755. [PubMed: 8393005]

50. Sabnis NA, Yang H, Romeo T. Pleiotropic regulation of the central carbohydrate metabolism in *Escherichia coli* via the gene *csrA*. J. Biol. Chem. 1995; 270:29096–29104. [PubMed: 7493933]

51. Yang H, Liu MY, Romeo T. Coordinate genetic regulation of glycogen catabolism and biosynthesis in *Escherichia coli* via the CsrA gene product. J. Bacteriol. 1996; 178:1012–1017. [PubMed: 8576033]

52. Romeo T. Post-transcriptional regulation of bacterial carbohydrate metabolism: evidence that the gene product CsrA is a global mRNA decay factor. Res. Microbiol. 1996; 147:505–512. [PubMed: 9084762]

53. Liu MY, Romeo T. The global regulator CsrA of *Escherichia coli* is a specific mRNA-binding protein. J. Bacteriol. 1997; 179:4639–4642. [PubMed: 9226279]

54. Wang X, Dubey AK, Suzuki K, Baker CS, Babitzke P, Romeo T. CsrA post-transcriptionally represses *pgaABCD*, responsible for synthesis of a biofilm polysaccharide adhesin of *Escherichia coli*. Mol. Microbiol. 2005; 56:168–1663.

55. Dubey AK, Baker CS, Suzuki K, Jones AD, Pandit P, Romeo T, Babitzke P. CsrA regulates translation of the *Escherichia coli* carbon starvation gene, *cstA*, by blocking ribosome access to the cstA transcript. J. Bacteriol. 2003; 185:4450–4460. [PubMed: 12867454]

56. Simon R, Priefer U, Pohler A. A broad host range mobilization system for *in vivo* genetic engineering: transposon mutagenesis in Gram-negative bacteria. Biotechnology. 1983; 1:784–791.

57. Haldimann A, Wanner BL. Conditional-replication, integration, excision, and retrieval plasmid-host systems for gene structure-function studies of bacteria. J. Bacteriol. 2001; 183:6384–6393. [PubMed: 11591683]

58. Sambrook, J.; Fritsch, EF.; Maniatis, T. Molecular Cloning: A Laboratory Manual. Cold Spring Harbor Laboratory; Cold Spring Harbor, NY: 1989.

59. Miller, JH. Experiments in Molecular Genetics. Cold Spring Harbor Laboratory; Cold Spring Harbor, NY: 1972.

60. Yakhnin AV, Trimble JJ, Chiaro CR, Babitzke P. Effects of mutations in the l-tryptophan binding pocket of the Trp RNA-binding attenuation protein of *Bacillus subtilis*. J. Biol. Chem. 2000; 275:4519–4524. [PubMed: 10660627]

61. Wang Y, Geer LY, Chappey C, Kans JA, Bryant SH. Cn3D: sequence and structure views for Entrez. Trends Biochem. Sci. 2000; 25:300–302. [PubMed: 10838572]

62. Yakhnin H, Pandit P, Petty TJ, Baker CS, Romeo T, Babitzke P. CsrA of *Bacillus subtilis* regulates translation initiation of the gene encoding the flagellin protein (*hag*) by blocking ribosome binding. Mol. Microbiol. 2007; 64:1605–1620. [PubMed: 17555441]

63. Hartz D, McPheeters DS, Traut R, Gold L. Extension inhibition analysis of translation initiation complexes. Methods Enzymol. 1988; 164:419–425. [PubMed: 2468068]
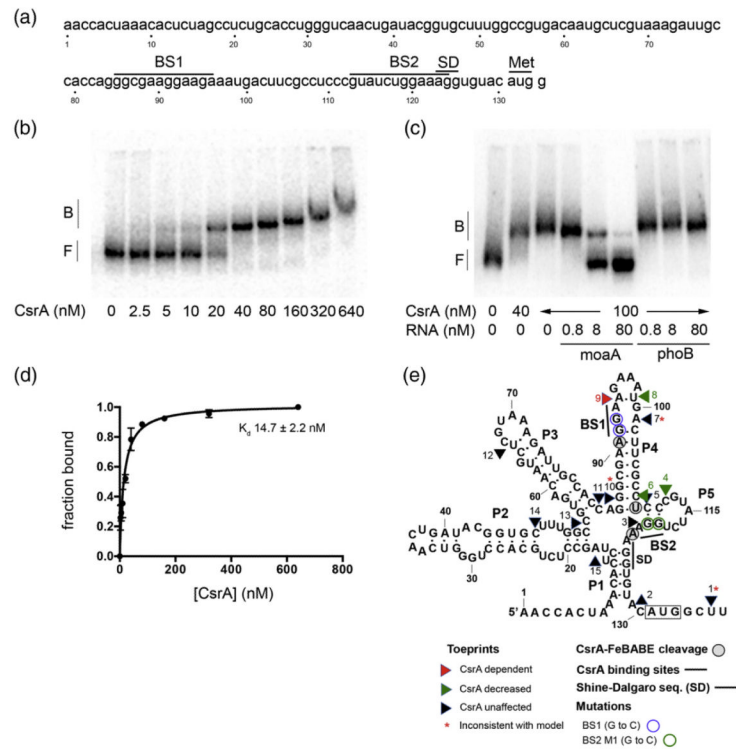
Fig. 1.
Gel mobility shift analyses of CsrA binding to *moaA* RNA and a secondary structure model summarizing the results of this study. (a) The *moaA* leader. The nucleotide sequence of the *moaA* leader used for gel shift analysis is shown. Putative CsrA binding sites (BS1 and BS2) are shown. The translation initiation site (Met) and the SD sequence are shown. (b and c) RNA gel mobility shift assays were performed to analyze the interactions between CsrA and the *moaA* leader. (b) Increasing concentrations of CsrA were incubated with ^{32}P-labeled *moaA* leader (80 pM). (c) RNA competition assays. Binding reactions were performed in the presence of unlabeled specific (*moaA* RNA) or nonspecific (*phoB* RNA) competitor. The positions of free (F) and bound (B) RNAs are shown. (d) Binding curve for the reaction shown in (b). (e) Structural model of *moaA* mRNA based on inline probing analyses.[41] Results of toeprinting, FeBABE footprinting and gel shift studies with base-substituted *moaA* RNAs in the CsrA binding sites (BS1 and BS2) are depicted on this structure.
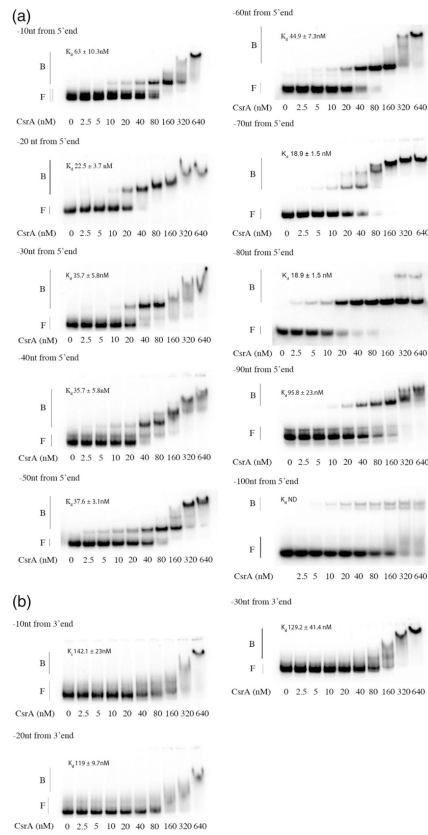
Fig. 2.
Deletion analysis of CsrA binding to *moaA* RNA. Labeled transcripts (80 pM) possessing deletions in 10-nt steps from the 5′ or the 3′ end of the *moaA* leader RNA (Fig. 1a) were incubated with increasing concentrations of CsrA, and the resulting complexes were examined in RNA gel shift studies. (a) 5′ deletions. (b) 3′ deletions. The positions of free (F) and bound (B) RNAs are shown.
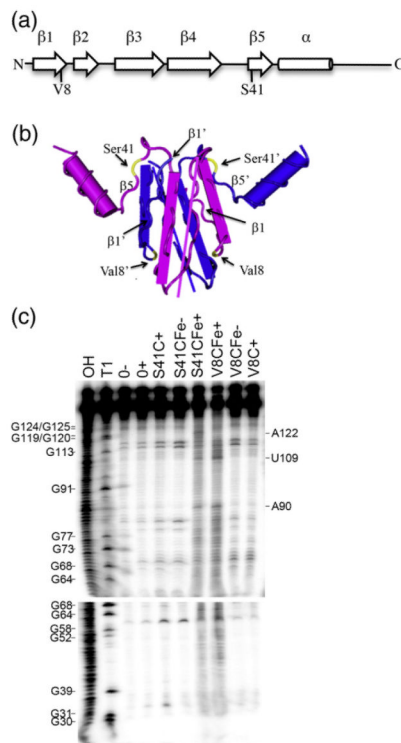
Fig. 3.
Footprinting of the *moaA* mRNA leader RNA with CsrA-FeBABE. (a) Cysteine residues were singly introduced at two different positions within the CsrA protein, valine 8 (V8C) or serine 41 (S41C), and derivatized with the FeBABE reagent. (b) The two polypeptides of the CsrA dimer are shown as blue or purple. Note that the $_1$ and $_5$ strands of opposite polypeptides of the dimer lie parallel with each other in the three-dimensional structure of the protein.[9] Residues Val8 and Ser41 are shown in yellow. (c) Footprinting of *moaA* leader RNA. ^{32}P-labeled *moaA* RNA was incubated with no CsrA (0), CsrA S41C (500 nM) or CsrA V8C (250 nM) in the absence (−) or presence (+) of cleaving reagents, ascorbic acid and hydrogen peroxide. OH and T1 indicate *moaA* RNA alkaline hydrolysis and partial RNase T1 ladders, respectively. Positions of strand scission are indicated on the right. Numbering is from the start of the *moaA* transcript shown in Fig. 1a.
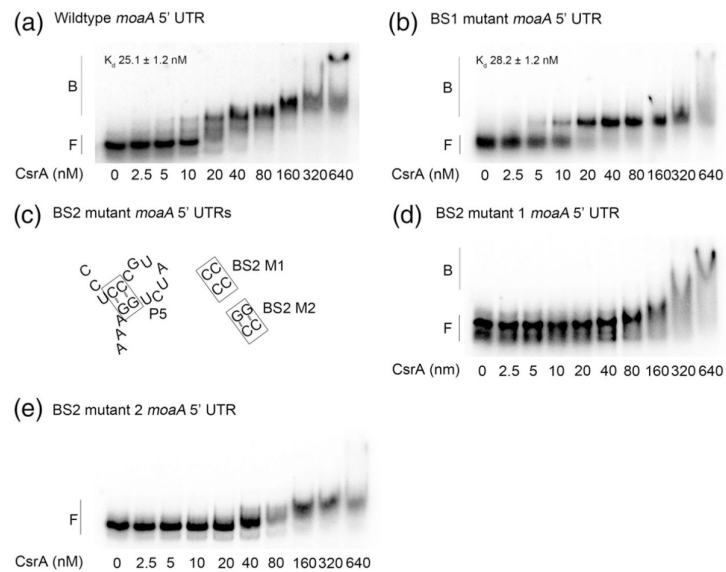
Fig. 4.
Effects of base substitutions in putative CsrA binding sites. Gel mobility shift assays were used to compare binding of CsrA to *moaA* leader transcripts containing GG-to-CC substitutions in putative CsrA binding sites identified by sequence analysis and FeBABE footprinting. (a) Gel shift with WT *moaA* leader RNA. (b) BS1-substituted RNA (NT 91–92; Fig. 1a). (c) Illustration of BS2 M1 substitutions (NT 119–120; Fig. 1a and e) and additional compensatory changes in BS2 M2 (NT 110–111) that restore base pairing. (d) Gel shifts with BS2 RNA. (e) Gel shifts with BS2 M2 RNA. The positions of free (F) and bound (B) RNAs are shown.
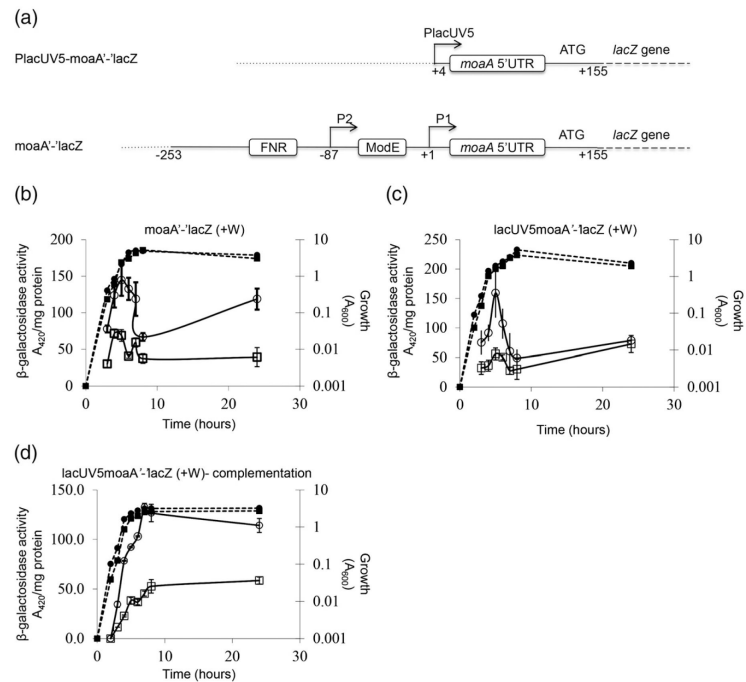
Fig. 5.
Effects of CsrA on expression of chromosomal *moaA'-'lacZ* and P*lacUV5-moaA'-'lacZ* fusions. (a) The P*lacUV5-moaA'-'lacZ* posttranscriptional fusion and the *moaA'-'lacZ* translational fusion are depicted. Binding sites for FNR and ModE transcription factors in the latter fusion are marked. Vector DNA (…) and the junctions between *moaA* DNA (—) and lacZ DNA (—) are also indicated. (b–d) For expression studies, cultures were harvested at various time points after inoculation (*T*=0) and assayed for -galactosidase specific activity (A_{420} per milligram of protein). Isogenic strains were from the CF7789 strain background. We added 10 mM sodium tungstate to derepress Moco-mediated regulation. Values represent independent experiments performed in triplicate, and error bars depict standard deviation of the mean. Growth (broken lines) and -galactosidase-specific activity (continuous lines) are presented. (b) Activity from a *moaA'-'lacZ* translational fusion. CF7789, ( ); *csrA*, (.). (c) Activity from a P*lacUV5-moaA'-'lacZ* posttranscriptional fusion. CF7789, ( ); *csrA*, (.). (d) Complementation analysis of expression from a P*lacUV5moaA'-'lacZ* fusion in a *csrA::kan* strain containing pBR322 (empty vector) (.) or the *csrA*-bearing plasmid pCRA16 ( ).
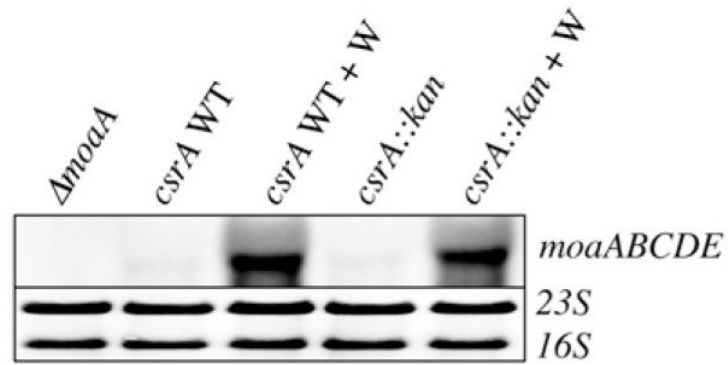
Fig. 6.
Northern analysis of *moaABCDE* mRNA in *csrA* WT and mutant strains. Total cellular RNA was isolated from the indicated *E. coli* strains, which were isogenic with CF7789. RNA (1 μg) was separated on a 1.2% formaldehyde agarose gel, transferred to a nylon membrane and hybridized with a DIG-labeled antisense *moaA* RNA probe. Sodium tungstate (20 mM) was added to eliminate Moco-mediated repression where indicated (+W). The 16S and 23S ribosomal RNAs served as loading controls.
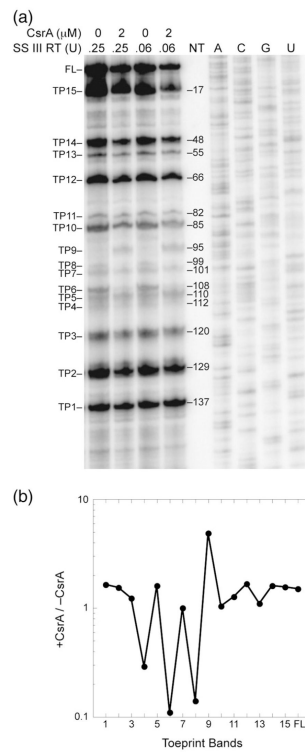
Fig. 7.
Toeprinting analysis of CsrA binding to *moaA* mRNA. (a) The absence or presence of CsrA (2 μM) and the amount of SuperScript III reverse transcriptase (SS III RT) is shown at the top of each lane. Each toeprint (TP) band is numbered with respect to its position *versus* the labeled primer. FL, full length. Sequencing reactions (A,C, G,U) for positioning the toeprints with respect to nucleotide sequence are also shown. The toeprinting positions are shown on a structural model for *moaA* RNA in Fig. 1e. (b) Quantification of the toeprint bands in lanes corresponding to 0.25 U reverse transcriptase. The intensity of each band was normalized to adjust for loading differences by dividing by the total intensity of each lane. Values of +CsrA/−CsrA are plotted with respect to each toeprint band. Bound CsrA caused a 3- to 10-fold.

Table 1

Strains, plasmids and bacteriophage

Strain, plasmid or phage	Description	Source or reference
Strain		
TRMG1655	MG1655 *csrA::kan*	43
CF7789	MG1655 *lacI-Z*(MluI)	Michael Cashel
TRBW3414	BW3414 *csrA::kan, rpoS*	43
PFLA881	CF7789 P*lacUV5-moaA* '-'*lacZ*	This study
TR PFLA881	PFLA881 *csrA::kan*	This study
PFA279	CF7789 *moaA* '-'*lacZ*	This study
TR PFA279	PFA279 *csrA::kan*	This study
S17-1 pir	*(pir) hsdRpro thi;* chromosomally integrated RP4-2 Tc::Mu Km::Tn7	56
BW25142	*lacI^q rrnB3 lacZ4787 hsdR514 DE(araBAD)567 DE(rhaBAD)568 phoBR580 rph-1 galU95 endA9 uidA(MluI)::pir*(wt) *recA1*	57
Plasmids		
pBR322	Cloning vector, Amp^r Tet^r	58
pCRA16	*csrA* in blunt-ended VspI site of pBR322	12
pLFT	Vector for translational fusions, Amp^r	14
pPFINT	Vector for integration, Tet^r	14
pUV5moaA	pLFT φ (P*lacUV5-moaA* '-'*lacZ*)	This study
pmoaA	pLFT φ (*moaA* '-'*lacZ*)	This study
pCSB12	*csrA* in NdeI and BamHI sites of pET21a+	5
pCSB12 X#C	*csrA* X#C C-terminal His_6-tag, derived from pCSB12	This study
pCSRH6-19	pKK223-3 expressing C-terminal His_6-tag CsrA, Amp^r	4
pCSRH6-19X#C	*csrA* X#C C-terminal His_6-tag, derived from pCSRH6-19	This study
pAlt-C4		48
pAltermoaA	*moaA* (LPF85:85) in EcoRI and BamHI sites of pAlter-1	This study
pAltermoaA (109:110) #2	pAltermoaA with mutations in *moaA* CsrA binding site BS2	This study
pAltermoaA (111:112) #1	pAltermoaA with mutations in *moaA* CsrA binding site BS2	This study
pAltermoaA (113:114) #2	pAltermoaA with mutations in *moaA* CsrA binding site BS1	This study
Bacteriophage		
P1 *vir*	Strictly lytic P1 for generalized transduction[59]	Carol Gross

Table 2

Oligonucleotide primers

Primer	Primer sequence (5′ to 3′)[a]	Application
Genetic techniques		
LPF-12	TTGTCGGTGAACGCTCTCCT	Sequencing pLFT fusions
LPF-13	AAGTTGGGTAACGCCAGG	Sequencing pLFT fusions
LPF-16	CT*GGATCC*AGTTGTGAAGCCATGTACAC	P*lacUV5-moaA* and *moaA-lacZ* translational fusions
LPF-17	AAGT*CTGCAG*CTCATTAGGCACCCCAGGCTTTACACTTT	P*lacUV5-moaA* translational fusion
	ATGCTTCCGGCTCGTATAATGTGTGGAACCACTAAACACTCTAGCCTC	
LPF-18	AAGT*CTGCAG*GAGTCAGATTATCCGCGCTACAGT	*moaA* translational fusion
LPF-85	AC*GAATTC*CACTAAACACTCTAGCGTC	Amplification of *moaA* (LPF 1:44) for cloning into pAlter-1
LPF-86	CT*GGATCC*CATGTACACCTTTCCAGATACGGGAGGCG	Amplification of *moaA* (LPF 1:44) for cloning into pAlter-1
ASmoaA T7fwd	<u>TAATACGACTCACTATAGGG</u>TTAGCCGCCAATGTACGA	*moaABCDE* antisense RNA probe
	TAAGTTTTGCGTAATACCGGTG	
ASmoaA T7rev	ATGGCTTCACAACTGACTGATGCATTTGCGCGTAAGTTTT	*moaABCDE* antisense RNA probe
M13for20	GTAAAACGACGGCCAGT	Sequencing
M13rev	AACAGCTATGACCATG	Sequencing
RNA EMSAs		
LPF-1	<u>TAATACGACTCACTATAGGG</u>CCACTAAACACTCTAGCCTC	Amplify full-length *moaA* riboswitch
LPF-2	TGCATCAGTCAGTTGTGAAGCCATGTACACC	Amplify full-length *moaA* riboswitch
LPF-42	<u>TAATACGACTCACTATAGGG</u>TGCACCTGGGTCAACTGATA	CsrA binding analysis (−20 nt from 5′ end)
LPF-43	AGTTGTGAAGCCATGTACACCTTTCCAGATAC	CsrA binding analysis (−10 nt from 3′ end)
LPF-44	CCATGTACACCTTTCCATATACGGGAGGCG	CsrA binding analysis (−20 nt from 3′ end)
LPF-45	<u>TAATACGACTCACTATAGGG</u>CTCTAGCCTCTGCACCTGGG	CsrA binding analysis (−10 nt from 5′ end)
LPF-46	TAATACGACTCACTATAGGGTCAACTGATACGGTGCTTTG	CsrA binding analysis (−30 nt from 5′ end)
LPF-47	<u>TAATACGACTCACTATAGGG</u>CGGTGCTTTGGCCGTGAC	CsrA binding analysis (−40 nt from 5′ end)
LPF-48	CTTTCCAGATACGGGAGGCGAAGTC	CsrA binding analysis (−30 nt from 3′ end)
LPF-49	ACGGGAGGCGAAGTCATTTCTTCC	CsrA binding analysis (−40 nt from 3′ end)
LPF-50	<u>TAATACGACTCACTATAGGG</u>GCCGTGACAATGCTCGTAAAG	CsrA binding analysis (−50 nt from 5′ end)
LPF-51	<u>TAATACGACTCACTATAGGG</u>TGCTCGTAAAGATTGCCACC	CsrA binding analysis (−60 nt from 5′ end)
LPF-52	<u>TAATACGACTCACTATAGGG</u>GATTGCCACCAGGGCG	CsrA binding analysis (−70 nt from 5′ end)
LPF-53	AAGTCATTTCTTCCTTCGCCCTGGTGG	CsrA binding analysis (−50 nt from 3′ end)

Primer	Primer sequence (5 to 3)[a]	Application
LPF-54	TTCCTTCGCCCTGGTGGCAATCTTTACG	CsrA binding analysis (−60 nt from 3 end)
LPF-55	CTGGTGGCAATCTTTACGAGCATTGTC	CsrA binding analysis (−70 nt from 3 end)
LPF-56	<u>TAATACGACTCACTATAGGG</u>CAGGGCGAAGGAAGAAATGAC	CsrA binding analysis (−80 nt from 5 end)
LPF-57	<u>TAATACGACTCACTATAGGGG</u>AAGAAATGACTTCGCC	CsrA binding analysis (−90 nt from 5 end)
GC LPF-57	TCCCGTATCTGGAAAGGTGTACATGG CCATGTACACCTTTCCAGATACGGGAGGCGAAGTCATTTCTT CCCCTATAGTGAGTCGTATTA	CsrA binding analysis (−90 nt from 5 end)
LPF-58	<u>TAATACGACTCACTATAGGG</u>TTCGCCTCCCG	CsrA binding analysis (−100 ntfrom 5 end)
GC LPF-58	TATCTGGAAGGTGTACATGG CCATGTACACCTTTCCAGATACGGGAGGCGAA CCCTATAGTGAGTCGTATTA	CsrA binding analysis (−100 ntfrom 5 end)
phoBT7-F	<u>TAATACGACTCACTATAGGGG</u>GCATTAATGATCG CAACCTATTTATTACAACAGGGCAAATCATG	*phoB* nonspecific competitor RNA
phoBT7-R	CATGATTTGCCCTGTTGTAATAAATAGGTTGCGA TCATTAATGC<u>CCCTATAGTGAGTCGTATTA</u>	*phoB* nonspecific competitor RNA
Site-directed mutagenesis		
LPF-63	GCCCCGAAGGAAGTT**TGC**GTTCACCGTGAAGAG	CsrA Ser41–Cys41 AA change; FeBABE
LPF-64	CTCTTCACGGTGAAC**GCA**AACTTCCTTCGGGGC	CsrA Ser41–Cys41 AA change; FeBABE
LPF-67	GAGCGGATAACAATTTCACACA	Sequencing; CsrA-His6 site-directed mutants (in pCSRH6-19)
LPF-68	TTCTCTCATCCGCCAAAACA	Sequencing; CsrA-His6 site-directed mutants (in pCSRH6-19)
LPF-89	CTGATTCTGACTCGTCGA**TGC**GGTGAGACCCTC	CsrA Val8–Cys8 AA change; FeBABE
LPF-90	GAGGGTCTCACC**GCA**TCGACGAGTCAGAATCAG	CsrA Val8–Cys8 AA change; FeBABE
LPF-109	AATGACTTCGCCT**GG**CGTATCT**CC**AAAGGTGTACATGG	Site-directed mutagenesis putative CsrA binding site
LPF-110	CCATGTACACCTTT**GG**AGATACG**CC**AGGCGAAGTCATT	Site-directed mutagenesis putative CsrA binding site
LPF-111	AATGACTTCGCCTCCCGTATCT**CC**AAAGGTGTACATGG	Site-directed mutagenesis putative CsrA binding site
LPF-112	CCATGTACACCTTT**GG**AGATACGGGAGGCGAAGTCATT	Site-directed mutagenesis putative CsrA binding site
LPF-113	GCCACCAGGGCGAA**CC**AAGAAATGACTTCGCC	Site-directed mutagenesis putative CsrA binding site
LPF-114	GGCGAAGTCATTTCTT**GG**TTCGCCCTGGTGGC	Site-directed mutagenesis putative CsrA binding site
LPF-115	GCCACCAGGGCGAA**CC**AAGAAATGA**G**TTCGCCTCCCGTATC	Site-directed mutagenesis putative CsrA binding site
LPF-116	GATACGGGAGGCGAA**C**TCATTTCTT**GG**TTCGCCCTGGTGGC	Site-directed mutagenesis putative CsrA binding site
Toeprinting		
T7 MoaA-For	GAAATAATACGACTCACTATAGGGCCACTAAACAC TCTAGCCTCTGCAC	PCR amplification to produce the template

Primer	Primer sequence (5′ to 3′)[a]	Application
		for *in vitro* transcription
LacZ2	GCTGGCGAAAGGGGGGATG	Primer for PCR amplification and the primer extension reaction

[a] Underlined nucleotides depict the T7 promoter sequence; italicized nucleotides show restriction enzyme cleavage sites; boldfaced nucleotides identify base substitutions. Sequences are shown in the 5′-to-3′ direction.